THE JOURNAL OF BIOLOGICAL CHEMISTRY
Vol. 277, No. 48, Issue of November 29, pp. 46385–46390, 2002
Printed in U.S.A.

Crystal Structure of Brain Pyridoxal Kinase, a Novel Member of the Ribokinase Superfamily*

Received for publication, August 22, 2002
Published, JBC Papers in Press, September 15, 2002, DOI 10.1074/jbc.M208600200

Ming-Hui Li‡, Francis Kwok§, Wen-Rui Chang‡, Chi-Kong Lau§, Ji-Ping Zhang‡, Samuel C. L. Lo§, Tao Jiang‡¶, and Dong-Cai Liang‡‖

From the ‡National Laboratory of Biomacromolecules, Institute of Biophysics, Chinese Academy of Science, Beijing 100101, China and §Department of Applied Biology and Chemical Technology, Hong Kong Polytechnic University, Hung Hom, Kowloon, Hong Kong, China

The three-dimensional structures of brain pyridoxal kinase and its complex with the nucleotide ATP have been elucidated in the dimeric form at 2.1 and 2.6 Å, respectively. Results have shown that pyridoxal kinase, as an enzyme obeying random sequential kinetics in catalysis, does not possess a lid shape structure common to all kinases in the ribokinase superfamily. This finding has been shown to be in line with the condition that pyridoxal kinase binds substrates with variable sizes of chemical groups at position 4 of vitamin B_6 and its derivatives. In addition, the enzyme contains a 12-residue peptide loop in the active site for the prevention of premature hydrolysis of ATP. Conserved amino acid residues Asp^{118} and Tyr^{127} in the peptide loop could be moved to a position covering the nucleotide after its binding so that its chance to hydrolyze in the aqueous environment of the active site was reduced. With respect to the evolutionary trend of kinase enzymes, the existence of this loop in pyridoxal kinase could be classified as an independent category in the ribokinase superfamily according to the structural feature found and mechanism followed in catalysis.

Pyridoxal-5′-phosphate (PLP)[1] is a key cofactor in the metabolism of amino acid. It catalyzes a large array of reactions in the synthesis, catabolism, and interconversion of amino acids (1). Mammals cannot synthesize PLP *de novo* and require its precursors in the form of vitamin B_6 (pyridoxal, pyridoxine, and pyridoxamine) from their diet. In the presence of Zn^{2+} and ATP, pyridoxal kinase (EC 2.7.1.35) catalyzes the phosphorylation of the precursor vitamins in tissues (2, 3) and plays a key role in the synthesis of the active coenzyme PLP (Fig. 1). PLP synthesized in liver is transported to other tissues through the blood stream. It must be dephosphorylated before gaining entry to target cells and rephosphorylated again by intracellular pyridoxal kinase after diffusion through cell membranes. PLP can be trapped and accumulated in the target cells by this mechanism. Consequently, there is a requirement for ubiquitous expression of pyridoxal kinase in mammalian tissues (4). Genes that encode pyridoxal kinase are also found in many other species including yeast and bacteria (5, 6).

PLP plays an important role in the nervous systems of mammals, as many neurotransmitters such as dopamine, norepinephrine, serotonin, and γ-aminobutyric acid are synthesized by PLP-dependent enzymes (7). Changes in PLP concentration in cells influence the stability of the nervous system. The side effects of many drugs that act upon the nervous system may be the result of alterations in pyridoxal kinase, leading to the fluctuation of the normal PLP concentration. This fluctuation breaks the equilibrium of neurotransmitter concentration and induces neurological disorders (8, 9). Drugs that inhibit pyridoxal kinase have been classified into three groups according to their different inhibitory mechanisms (10).

A model for transporter-enhanced delivery of bioactive compounds has been proposed based on the broad specificity of pyridoxal kinase. In this model, a drug or other intracellular effector bearing an amine functional group gains facilitated entry into cell after it forms a stable transportable compound with pyridoxal, and then it is liberated by the intracellular pyridoxal kinase and pyridoxine-5′-phosphate (11).

Pyridoxal kinases have been purified from different tissues, and several genes that encode pyridoxal kinase have also been determined. Properties of the substrate-binding sites have been explored by using different inhibitors (12, 13). Some essential residues in the proximity of the enzyme active site have been determined with chemical modification methods (14–16). The arrangement of substrates at the active site was also studied by means of fluorescence and NMR spectroscopy (17, 18). Although crystallization and preliminary crystallography studies in the trigonal form have been reported (19), the three-dimensional structure of pyridoxal kinase was not known. Pyridoxal kinase from sheep brain is a homodimer with each monomer containing 312 amino acid residues. The dimer can dissociate reversibly into catalytically active monomers (20). The inhibition kinetic patterns of the reaction catalyzed by pyridoxal kinase are consistent with a rapid equilibrium random BiBi mechanism (21).

In this article, we describe the three-dimensional structures of both pyridoxal kinase and its enzyme-ATP complex. The crystal structure of pyridoxal kinase reveals that the enzyme is being classified as a member of the ribokinase superfamily (22).

* This project was supported by grants from the National Natural Science Foundation of China (30100026), Life Science Special Fund of the Chinese Academy of Science (STZ0017), and National Key Research Development Project of China (G1999075601). The costs of publication of this article were defrayed in part by the payment of page charges. This article must therefore be hereby marked "*advertisement*" in accordance with 18 U.S.C. Section 1734 solely to indicate this fact.

The atomic coordinates and structure factors for pyridoxal kinase (code 1LHP) and its complex with ATP (code 1LHR) have been deposited in the Protein Data Bank, Research Collaboratory for Structural Bioinformatics, Rutgers University, New Brunswick, NJ (http://www.rcsb.org/).

¶ To whom correspondence may be addressed: 15 Datun Rd., Chaoyang District, Beijing 100101, China. Tel.: 86-10-64888510; Fax: 86-10-64889867; E-mail: x-ray@sun5.ibp.ac.cn.

‖ To whom correspondence may be addressed: 15 Datun Rd., Chaoyang District, Beijing 100101, China. Tel.: 86-10-64888506; Fax: 86-10-64889867; E-mail: dcliang@sun5.ibp.ac.cn.

[1] The abbreviations used are: PLP, pyridoxal-5′-phosphate; MES, 4-morpholineethanesulfonic acid; THZ, 4-methy-5-β-hydroxyethylthiazole; HMPP, 4-amino-5-hydroxymethyl-2-methylpyrimidine phosphate.

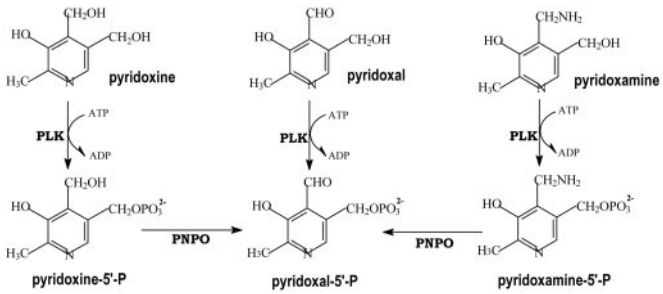

FIG. 1. **Synthesis of PLP from vitamin B_6.** *PLK*, pyridoxal kinase; *PNPO*, pyridoxine-5′-phosphate oxidase.

Compared with other kinases in this superfamily, brain pyridoxal kinase has some unusual features. It does not contain a lid-shaped structure that is common in other kinases. This new feature is designed to accommodate many substrates, which include all three forms of vitamin B_6 (pyridoxal, pyridoxine, and pyridoxamine) as well as other B_6 analogues (2, 3, 11). On the other hand, brain pyridoxal kinase follows an unusual random mechanism of substrate addition (21) rather than the ordered one for which the structural basis had been elucidated in detail by early studies on ribokinase and adenosine kinase (22–24). Our current studies on a loop present in pyridoxal kinase provide the first structural explanation for the random mechanism in this superfamily. An evolutionary pathway has been suggested for the kinases in ribokinase superfamily based on the morphological difference of an active site lid (25), whereas the structure and properties of pyridoxal kinase indicate a new category evolutionary development in this superfamily.

EXPERIMENTAL PROCEDURES

Purification, Crystallization, and Data Collection—Pyridoxal kinase was isolated and purified from sheep brain as described (1). Crystals of pyridoxal kinase were grown by the hanging-drop vapor-diffusion method as reported previously (26). The protein concentration was adjusted at 10 mg ml^{-1} in 0.1 M sodium citrate, pH 5.8. The enzyme solution was mixed in equal volumes with 1.1 M sodium citrate, pH 5.8, and equilibrated against this solution at 17 °C. After 1 month, crystals were grown until final dimensions were reached. The crystals belong to the space group $P2_12_12_1$ with $a = 59.8$ Å, $b = 94.4$ Å, $c = 128.2$ Å. They were transferred to a mother liquid consisting of 20% polyethylene glycol 8000, 0.1 M Na_2SO_4, and 50 mM MES buffer, pH 6.0, and then heavy atom soaks were performed. The enzyme-ATP complex was obtained by soaking crystals overnight in a solution containing 1 mM ATP, 1 mM zinc acetate, 30% polyethylene glycol 6000, and 75 mM KH_2PO_4-K_2HPO_4, pH 6.5.

All data were collected at room temperature. The native data sets were collected with a Weissenberg camera on Beamline BL6B at the Photon Factory (Tsukuba, Japan). The data sets from heavy atom derivatives of pyridoxal kinase and the pyridoxal kinase-ATP complex were collected using the MAR345 image plate in the National Laboratory of Biomacromolecules (Beijing, China). All data were processed using DENZO and SCALEPACK (27). Statistics for the data are shown in Table I.

Structure Determination—The native structure of pyridoxal kinase was solved by the multiple isomorphous replacement method. Positions of heavy atoms were located using the CCP4 program suit. The program MLPHARE (28) was used to refine the parameters of heavy atoms and to calculate the initial phase at 2.9 Å. The noncrystallographic 2-fold axis was determined using the program FINDNCS (29). Solvent flattening and density averaging was carried out using DM (30). The density map obtained was sufficiently clear to build an initial model using the program O (31); the model included most of the residues except those in two loops and the N-terminal four residues of the two monomers. Refinement was carried out using the program CNS (32) with restrained 2-fold noncrystallographic symmetry in the starting stage, and the resolution was extended to 2.1 Å. A model was rebuilt manually according to a composite omit density map. After several cycles of refinement and rebuilding, as well as the addition of 211 water molecules, a final model with an R-factor of 0.195 and an R_{free} of 0.224 was reached (Table I). Assessment of the final model using the program PROCHECK (33) showed that 92.7% of the residues were in the most favorable region and no residue were in the disallowed region.

The structure of the pyridoxal kinase-ATP complex was solved by the difference Fourier method using the native structure as the model. After rigid body refinement of the two monomers in the asymmetric unit, the calculated $F_o - F_c$ map clearly displayed the density of the ATP molecules (Fig. 5, *a* and *b*). The model was refined using the CNS program and rebuilt using an omit density map. The final R-factor was 0.196, and the R_{free} was 0.225 (Table I).

RESULTS AND DISCUSSION

Overall Structure—The three-dimensional structure of pyridoxal kinase has revealed that there are two identical monomers related by a noncrystallographic 2-fold axis in the asymmetric unit (Fig. 2*a*). Each monomer contains 9 α-helices, 10 β-strands, and 3 segments of 3_{10} helices. The 10 β-strands form a central β-sheet flanked by α2, α3, α4, α5, α6 on one side and α1, α7, α8, α9 on the other side. This fold is similar to the core structure of the ribokinase superfamily (Fig. 2, *b* and *c*), which includes ribokinase (22), human adenosine kinase (34), adenosine kinase from *Toxoplasma gondii* (24), 4-methy-5-β-hydroxyethylthiazole (THZ) kinase (35), ADP-specificity glucokinase (36), and the recently reported 4-amino-5-hydroxymethyl-2-methylpyrimidine phosphate (HMPP) kinase (25). Despite the structural similarity, the amino acid identity between pyridoxal kinase and any of these kinases is low, and only part of the sequence can be aligned. The structure of pyridoxal kinase represents a new family in this superfamily. Superimposition of the three-dimensional structures results in only 191 of 312 residues of pyridoxal kinase being structurally equivalent to the residues in HMPP kinase with a root-mean-square distance of 2.2 Å for the Cα atoms.

The dimeric structure of pyridoxal kinase is formed by the two monomers in asymmetrical unit through hydrogen bonding and salt bridges as well as hydrophobic interactions between the α1, α9, β1, and β3 of both monomers. The buried area of the two monomers is 3860 $Å^2$, and each monomer contributes about 1930 $Å^2$ corresponding to 13.6% of the total area of one monomer. Each monomeric unit of pyridoxal kinase contains an active site, which does not overlap in the interface of monomers (Fig. 2*a*). Biochemical studies on pyridoxal kinase also showed that the dissociating monomer of this enzyme retained activity (20). The biological implications for dimerization of pyridoxal kinase is still not clear from the structural point of view. In addition, there is no evidence concerning possible cooperativity or allosteric control of this kinase between subunits.

ATP-binding Site—The structure of the pyridoxal kinase-ATP complex reveals that each monomer binds an ATP molecule. After binding to the protein, ATP is located in a shallow groove formed by the ends of β strands β6, β7, β8, and β9 and helices α7 and α8 on the enzyme surface (Fig. 4, *c* and *d*). The location of the shallow groove is consistent with a previous report on its shape as viewed by electronic microscopy (1). Superimposition of the enzyme in the absence of ATP and the enzyme-ATP complex reveals that all of the main chain conformations except those residues from B117 to B128 of pyridoxal kinase show little change upon binding of ATP (Fig. 4*b*). In the ATP-binding site, we observed that only the side chain of Met^{233} changes its position, to avoid close contact with ATP. The residues that interact with ATP are shown in Fig. 3*a*. The adenine ring and ribose of ATP are partially buried in a pocket formed by the hydrophobic side chains of surrounding residues. There are two direct hydrogen bonds between the base of ATP (N-1 and N-6) and the protein (the main chain N and O atom in residue Thr^{226}) and an indirect hydrogen bond between the N-7 of the base and the main chain N atom of Phe^{229} via a water molecule. The phosphate groups of ATP form hydrogen bonds

TABLE I
Structure determination and refinement
PCMS, *p*-chloromercuriphenylsulfonic acid derivative; PLK, pyridoxal kinase; r.m.s., root-mean-square.

	Native	K_2PtCl_6	PCMS	CH_3HgCl	K_2HgI_4	PLK-ATP
Data collection statistics[a]						
Resolution, Å	20–2.1	20–2.9	20–2.9	20–3.0	20–3.0	20–2.6
Reflections, observed/unique	182,984/42,820	107,721/16,461	117,789/16,605	103,347/15,071	103,588/14,983	102,919/22,649
Completeness, %	99.1 (98.7)	100.0 (100.0)	99.9 (100.0)	99.7 (100.0)	100.0 (100.0)	99.9 (99.7)
R_{merge}, %[b]	6.6 (35.3)	13.5 (48.4)	13.5 (47.4)	13.6 (49.5)	16.4 (55.2)	12.4 (61.7)
Mean (I/σ(I))	20.4 (4.1)	14.2 (3.8)	15.7 (4.5)	14.7 (4.0)	12.6 (3.4)	12.0 (2.2)
Phasing statistics						
R_{deriv}, %		16.9	17.3	29.2	26.0	
Number of sites		4	4	8	9	
R_{cullis}, acentric/centric[c]		0.85/0.78	0.81/0.66	0.66/0.65	0.77/0.70	
Phasing power, acentric/centric[d]		1.09/0.89	1.40/1.24	1.85/1.38	1.45/1.21	
Overall figure of merit				0.53		
Refinement statistics						
Resolution, Å	20–2.1					20–2.6
R_{work}/R_{free}, %[e]	19.5/22.4					19.6/22.5
r.m.s. deviation						
Bond lengths, Å	0.008					0.008
Bond angles, °	1.3					1.3
Mean B-factor, Å^2						
Main chain	28.1					31.3
Side chain	31.1					33.3
Solvent	36.9					34.9

[a] Statistics for the highest resolution bin are in parentheses.
[b] $R_{merge} = \Sigma_h \Sigma_i | I(h,i) - <I(h)> | / \Sigma_h \Sigma_i I(h,i)$, where $I(h,i)$ is the intensity of the ith measurement of the reflection h and $<I(h)>$ is the mean value of the $I(h,i)$ for all I measurements.
[c] $R_{cullis} = \Sigma \| F_{PH}| \pm | F_P| - | F_{H(calc)} \| / \Sigma | F_{PH} | \pm | F_P \|$.
[d] Phasing power = $<F_H>/<$lack of closure$>$.
[e] R_{free} was calculated with 5% of data.

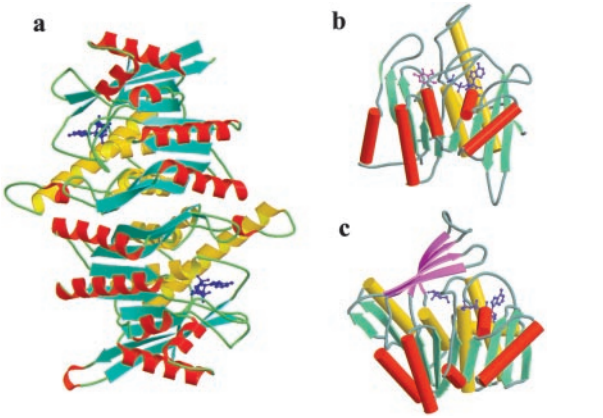

FIG. 2. **Structure of pyridoxal kinase.** *a*, dimeric structure of pyridoxal kinase viewed along the 2-fold axis. The *blue* molecule is ATP. *b* and *c*, the monomer structures of pyridoxal kinase and ribokinase. Their common secondary structures are in the same colors (*red*, *green*, and *yellow*). The lid in ribokinase that does not exist in pyridoxal kinase is in *magenta*. ATP, AMP-PCP, and ribose molecules are shown in *blue* and the modeled pyridoxal in *magenta*. This figure and all following figures were generated using MolScript (38), Raster3D (39), GRASP (40), or TURBO-FRODO (41).

with protein directly or through solvent molecules. Residues that interact with the phosphate groups are Ser^{187}, Thr^{148}, Asp^{113}, Asn^{150}, Asp^{118}, Gly^{234}, Tyr^{127}, and Thr^{233}. They are highly conserved in the primary sequences of pyridoxal kinase among different species. A Zn^{2+} ion and a K^+ ion are found together with an ATP molecule in the active site. The Zn^{2+} ion binds to the oxygen atoms of both the β- and γ-phosphate groups of ATP, but it does not interact directly with the protein. In general, the Mg^{2+} ion is commonly used in reactions catalyzed by kinases. Brain pyridoxal kinase, however, exhibits strikingly higher activity in the presence of Zn^{2+} than Mg^{2+} (2, 13). As interaction between Zn^{2+} and the protein was not observed in the enzyme-ATP complex, this preference for Zn^{2+} may result from the succeeding steps of catalytic reactions. The coordination of the K^+ ion is octahedral, and its ligands are atoms of the β-phosphate group, the surrounding residues (Thr^{186}, Thr^{148}, Asp^{113}, and Glu^{153}), and a water molecule. Those residues located in this site make it possible for the K^+ ion to engage in the binding of ATP, which corresponds to the activation of K^+ ion on pyridoxal kinase (37).

A Loop in the Active Site—According to structural analysis, the pyridoxal-binding site should be in close proximity to the γ-phosphate group of ATP. Nevertheless, in the absence of ATP, the pyridoxal-binding site of each monomer is occupied by a 12-residue loop (117–128) connecting β5 and α4 (Fig. 4*a*). Such a loop has never been observed in ribokinase, adenosine kinase, THZ kinase, and ADP-specificity glucokinase. In the similar location of HMPP kinase, a relatively shorter loop takes part in the formation of a nascent lid covering the substrate HMP (25). In brain pyridoxal kinase, not only is the loop longer than the loop present in HMPP kinase but it also penetrates deeply to the inner core of the protein molecule and occupies the pyridoxal-binding site completely, leaving no space for the substrate. Because of the broad substrate specificity of pyridoxal kinase (2, 3, 11), it is suggested that this loop cannot perform the same function as that in HMPP kinase. In the pyridoxal kinase-ATP complex, the loop of monomer A is restricted by the other symmetrical molecule in the crystal and remains unchanged from the native structure (Fig. 4, *b* and *c*). However, the loop in monomer B, which is in contact with the solvent region of the crystal without any lattice limitation, swayed completely to another direction, partially covering the ATP (Fig. 4, *b* and *d*) and leaving the pyridoxal-binding site exposed to the solution environment. Based on its random mechanism (21), pyridoxal kinase can bind vitamin B_6 before ATP. Therefore, it is expected that when vitamin B_6 binds to the enzyme before ATP binds to the protein, this loop will display a conformation that neither occupies the pyridoxal-binding site nor covers the ATP-binding site.

Pyridoxal-binding Site—After binding ATP, loop-(117–128) of monomer B sways out of its original position and leaves the pyridoxal-binding site exposed, forming a cavity with negative charges next to the ATP-binding site on the surface of pyridoxal

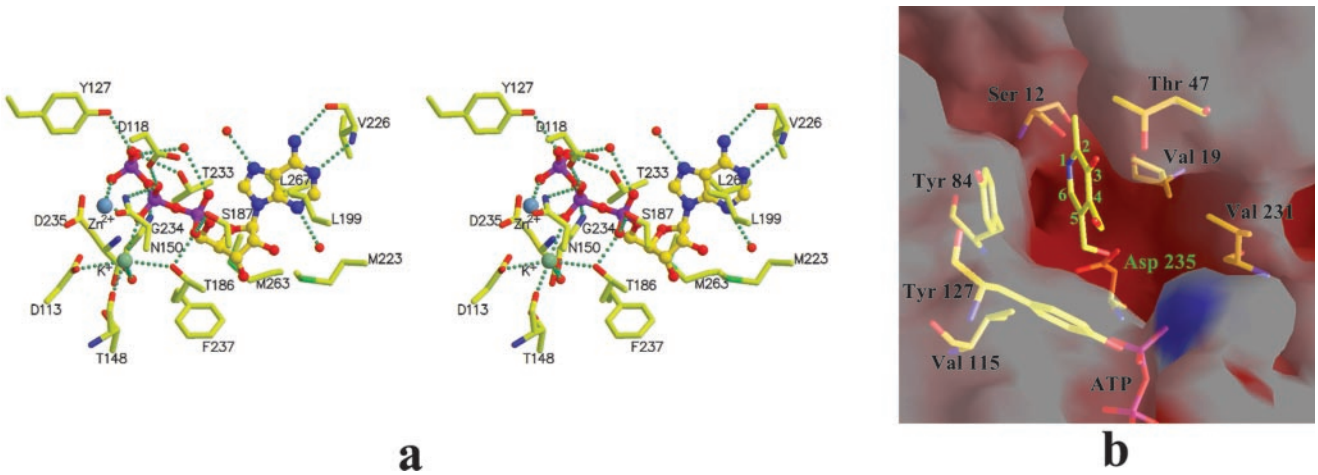

FIG. 3. **Substrate-binding sites of pyridoxal kinase.** *a*, stereoview of the interactions between ATP and residues of enzyme in the complex. The bound ATP molecule is shown as a *ball-and-stick* model; Zn^{2+} and K^+ are shown as *spheres*. *b*, the pyridoxal-binding site is shown as a *transparent* electrostatic surface. Positive regions are *blue*, and negative regions are *red*; the modeled pyridoxal and related residues are shown as *sticks*. The positions of the pyridine ring of pyridoxal are labeled.

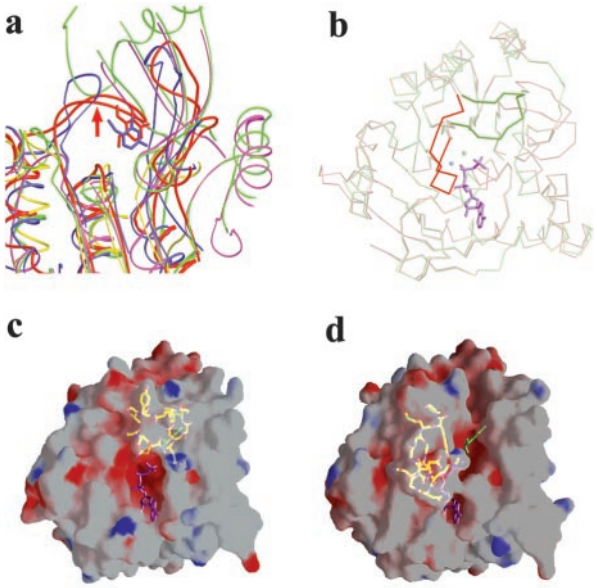

FIG. 4. **The active site loop.** *a*, superimposition of the local structures of kinases in ribokinase family. Pyridoxal kinase, *red*; adenosine kinase, *green*; ribokinase, *magenta*; thiazole kinase, *yellow*; and HMPP kinase, *blue*. The *red* molecule is pyridoxal, and the *blue* one is HMPP. The *red arrow* shows the active site loop in pyridoxal kinase. *b*, superimposition of two monomers of pyridoxal kinase-ATP complex reveals that the loops have two different conformations. Monomer A is *red*, and monomer B is *green*. The *magenta* molecule represents ATP, and *white balls* represent Zn^{2+} and K^+. *c* and *d*, molecular surface of two monomers of pyridoxal kinase-ATP complex. In monomer B, the pyridoxal-binding site is exposed. The residues in the loop taking different conformations are shown in *yellow*. ATP is in *magenta* and modeled pyridoxal in *green*.

kinase (Figs. 3*b* and 4*d*). The high negative potential of this site is favorable to the binding of substrates because of the attraction created by the positive charge on the pyridine ring of vitamin B_6. It is also suggested that the more positive charges a substrate has, the more readily it will bind to the enzyme. As concerns the three chemical forms of vitamin B_6, the K_m of pyridoxamine with two positive charges is 0.006 mM, which is lower than the K_m of pyridoxal (0.04 mM) and pyridoxine (0.026 mM) (1). Here, a pyridoxal-binding model for pyridoxal kinase is hypothesized (Fig. 3*b*). In this model, Tyr^{84} is on one side of the pyridine ring of pyridoxal and makes an π-interaction with the pyridine ring, whereas Val^{231} and Val^{19} are on the other side interacting hydrophobically with pyridoxal. This hypothesis is supported by previous chemical modification studies in which a Tyr residue was shown to be essential for the binding of pyridoxal to the kinase (15). The N-1, O-3, and O-5 atoms of pyridoxal form hydrogen bonds with the side chains of Ser^{12}, Thr^{47}, and Asp^{235}, respectively. Furthermore, residues Val^{41}, Phe^{43}, Val^{14}, Val^{56}, Trp^{52}, and Val^{115} all contribute to form a hydrophobic environment for the binding of pyridoxal to the active site. All of these residues, especially Tyr^{84}, Asp^{235}, and Ser^{12}, share the function of determining substrate specificity and are highly conserved among pyridoxal kinases. Another role of Asp^{235} is to attract the proton of the 5′-hydroxyl group of pyridoxal; the negatively charged oxygen atom makes a nucleophilic attack on the γ-phosphate group of ATP in the catalytic reaction.

The Absence of a Lid Structure in the Active Site—Biochemical studies have shown that pyridoxal kinase can tolerate considerable variation with respect to the size and chemical nature of a group at position 4 of a pyridoxal derivative (2, 3). The size of a chemical group at this position may vary from being an hydroxyl as shown in pyridoxine to pyridoxyl derivatized with benzylamine and tryptamine (11). According to the pyridoxal-binding model, based on our finding, the 4′-substitute group of the pyridoxal derivatives appears not to interact with any residue of the protein and points to the solvent region. The tolerance for the variation of this chemical group would not allow any peptide chain to cover the binding site as a lid structure to create hindrance to the binding process. In this respect, pyridoxal kinase is shown to be significantly different from the other kinases as compared with those enzymes in the ribokinase superfamily. All of the other kinases contain a lid structure covering the bound substrates. In ribokinase (22), adenosine kinase (24, 34) and ADP-dependent glucokinase (36), a small domain of the enzyme structure forms this lid structure. However, in the trimeric structure of THZ kinase, each monomer plays the role of the lid for the adjacent monomer (35), and in HMPP kinase, a nascent lid formed by a flexible loop and two β-strands exists (25).

Structural studies on adenosine kinase, ribokinase, and their complexes with substrates or ATP analogues have given an explanation of the function of their lids (22, 23, 24). Initially, the lids (a small domain) are in the opening state of the enzyme, enabling the entrance of ribose or adenosine to their binding sites. Before ATP binding to the kinase, the binding of the first substrate induces a conformational change of the

protein structure by rotating the lid toward a site where the first substrate has been bound. This movement results in the covering and tight trapping of the first substrate in the correct position for catalysis. Furthermore, the rotating movement of the lids together with other local conformational adjustments makes these kinases more favorable to binding ATP. Typically, the lid of adenosine kinase rotates about 30° upon the binding of adenosine, and a positively charged residue, Arg^{136}, is translocated for a distance of 13.6 Å to the binding site of ATP. This translocation promotes the correct positioning and stabilization of the negatively charged phosphate group on ATP (24). The purpose of such a mechanism in substrate binding has been suggested as the prevention of premature ATP hydrolysis (22).

The absence of such a lid in the structure of brain pyridoxal kinase indicates that pyridoxal kinase binds its substrates differently than ribokinase and adenosine kinase. Kinetic data for brain pyridoxal kinase were consistent with a random binding of substrates (21) in which ATP is able to bind to pyridoxal kinase before binding vitamin B_6, which is also confirmed by the crystallization of ATP-kinase complex in the absence of vitamin B_6. In addition, it is found that the pyridoxal-binding site is exposed after ATP binds to the enzyme. When ATP binds to the kinase in the absence of pyridoxal, securing the nonexistence of premature hydrolysis of ATP may become a crucial element for the random sequential kinetic mechanism.

The Relationship between the Loop in the Active Site and the Prevention of ATP Hydrolysis—It has been found that in the structure of pyridoxal kinase-ATP complex, the electron density of ATP bound in monomer A at the γ-phosphate group is weaker than at α- and β-phosphate groups (Fig. 5*a*). This suggests that this ATP has been hydrolyzed in considerable proportion. In monomer B, the three phosphate groups of ATP all fit the density well (Fig. 5*b*). The observation that there is little difference between the two monomers in the active sites except the conformation of loop-(117–128) reveals that one function of this loop may be to prevent premature ATP hydrolysis before binding of vitamin B_6. A common catalytic mechanism has been suggested for the ribokinase superfamily (24). In this mechanism, the hydroxyl group of the phosphate accepter is activated by a basic group in the active site, and then its oxygen atom makes a direct nucleophilic attack to the γ-phosphate group of ATP in an in-line mechanism and breaks it off. In the structures of adenosine kinase-adenosine-AMPPCP complex and ribokinase-ribose-AMPPCP complex, the arrangement of the substrates allows the hydroxyl oxygen atoms to attack the γ-phosphate group in the proper ways (Fig. 5*c*). In pyridoxal kinase, there is a water molecule between the γ-phosphate of ATP and the carboxyl group of Asp^{235}, the basic catalytic group. However, this water is located close to the plane of the three oxygen atoms of the γ-phosphate group (Fig. 5*c*), from where the water cannot make a nucleophilic attack in the manner mentioned above. The occurrence of hydrolysis requires conformational changes on ATP to make the γ-phosphate group move toward the water. However, when monomer B binds ATP, the conformation of loop-(117–128), as discussed above, allows the hydroxyl group of Tyr^{127} to form a hydrogen bond with the γ-phosphate group of ATP. At the same time the side chain of Asp^{118} makes a hydrogen bond with the β-phosphate group. The two additional hydrogen bonds restrict the conformation of ATP, which keeps the γ-phosphate in a conformation from which ATP hydrolysis is prevented. The loop of monomer A was fixed by crystal packing, and its conformation did not allow these two residues to interact with ATP. Thus, ATP hydrolysis was not prevented. In summary, the conformational variation of loop-(117–128) and the restriction on ATP

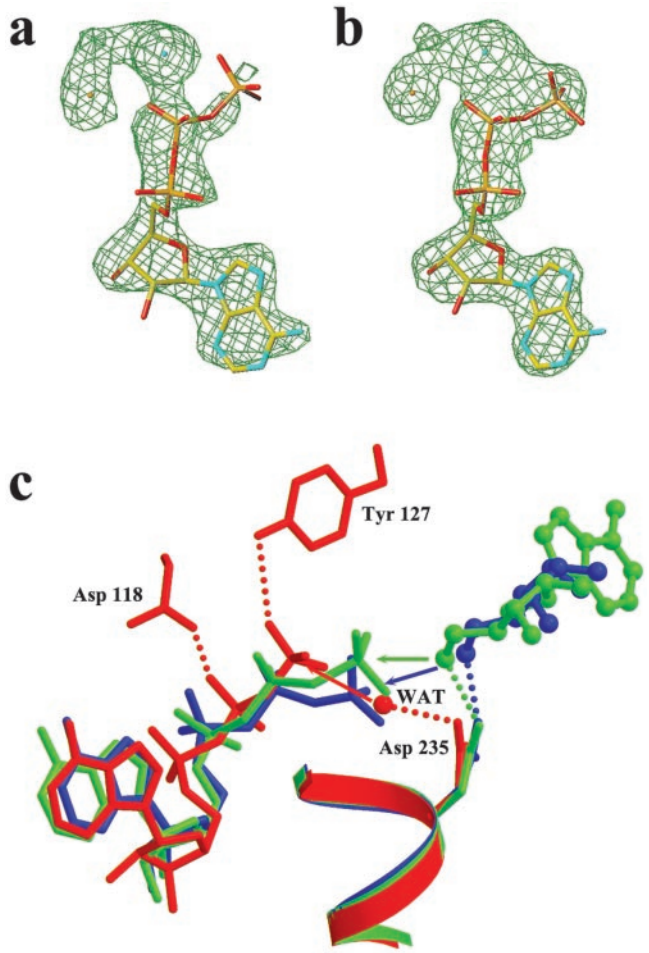

FIG. 5. *a* and *b*, omit electron density maps of the ATP molecules bound in the complex in monomer A (*a*) and monomer B (*b*). *c*, a superimposed view of the active site of pyridoxal kinase (*red*), ribokinase (*blue*), and adenosine kinase (*green*). The superimposition is based on the common catalytic residue Asp and the helix to which it belongs.

exerted by Asp^{118} and Tyr^{127} are essential to prevent premature ATP hydrolysis in the random binding mechanism of catalysis.

Different Sequences and Functions of the Loop—Sequences alignment of 29 pyridoxal kinases has shown that Asp^{118} and Tyr^{127} are conserved in 21 sequences (data not shown), which also shows their importance. Interestingly, in 6 of the remaining 8 sequences, these two residues change to His and Val/Ile simultaneously, suggesting that there is another type of pyridoxal kinase as a result of the difference of the loop. Two pyridoxal kinase genes (*pdxK* (5) and *pdxY* (6)) have been found in *Escherichia coli*. These two residues in *pdxK* are Asp and Tyr, the same as found in brain pyridoxal kinase. Enzyme expressed from this gene can use all pyridoxal, pyridoxine, and pyridoxamine as substrates (5). The other gene, *pdxY*, with His and Ile at the two sites, has a far lower activity level when using pyridoxine rather than pyridoxal as a substrate (6), indicating that this enzyme interacts with the 4′-substituted substrate group and limits its chemical nature. This evidence demonstrates that the loops in the two types of pyridoxal kinases have different functions during reactions. The Asp-Tyr loop plays a role similar to that of the loop in brain pyridoxal kinase, which interacts with ATP and prevents ATP hydrolysis; whereas the His-Val/Ile loop plays a role similar to that of the loop in HMPP kinase at the comparable position, which acts as a lid and covers the bound non-ATP substrate.

An evolutionary pathway has been proposed for known struc-

tures in ribokinase superfamily according to the morphological differences in the lid structures (25). Brain pyridoxal kinase does not have such a lid. Furthermore, compared with the loop in HMPP kinase, which forms a nascent lid with the other two β-strands together, the loop in pyridoxal kinase possesses two significantly conserved residues that interact with ATP, which endows the loop with a new function (preventing ATP hydrolysis), and adapts pyridoxal kinase to a new mechanism (random sequential kinetic mechanism). This suggests another evolutionary direction for the proteins in the ribokinase superfamily and also provides a typical case for how the enzyme adapts to a mechanism by local structural changes while retaining the core structure of the protein macromolecule.

Acknowledgments—We thank Prof. N. Sakabe and Dr. K. Sakabe of the Photon Factory for help in collecting data.

REFERENCES

1. Kerry, J. A., Rohde, M., and Kwok, F. (1986) *Eur. J. Biochem.* **158,** 581–585
2. McCormick, D. B., and Snell, E. E. (1959) *Proc. Natl. Acad. Sci. U. S. A.* **45,** 1371–1379
3. McCormick, D. B., and Snell, E. E. (1961) *J. Biol. Chem.* **263,** 2085–2088
4. Hanna, M. C., Turner, A. J., and Kirkness, E. F. (1997) *J. Biol. Chem.* **272,** 10756–10760
5. Yang, Y., Zhao, G., and Winkler, M. E. (1996) *FEMS Microbiol Lett.* **141,** 89–95
6. Yang, Y., Tsui, H. C., Man, T. K., and Winkler, M. E. (1998) *J. Bacteriol.* **180,** 1814–1821
7. Dakshinamurti, K., Paulose, C. S., Viswanathan, M., Siow, Y. L., Sharma, S. K., and Bolster, B. (1990) *Ann. N. Y. Acad. Sci.* **585,** 128–144
8. Ubbink, J. B., Vermaak, W. J., Delport, R., Serfontein, W. J., and Bartel, P. (1990) *Ann. N. Y. Acad. Sci.* **585,** 285–294
9. Shetty, K. T., and Gaitonde, B. B. (1980) *Exp. Neurol.* **70,** 146–154
10. Laine-Cessac, P., Cailleux, A., and Allain, P. (1997) *Biochem. Pharmacol.* **54,** 863–870
11. Zhang, Z. M., and McCormick, D. B. (1991) *Proc. Natl. Acad. Sci. U. S. A.* **88,** 10407–10410
12. Kwok, F., and Churchich, J. E. (1979) *Eur. J. Biochem.* **93,** 229–235
13. Churchich, J. E., and Wu, C. (1982) *J. Biol. Chem.* **257,** 12136–12140
14. Kwok, F., and Churchich, J. E. (1979) *J. Biol. Chem.* **254,** 6489–6495
15. Scholz, G., and Kwok, F. (1989) *J. Biol. Chem.* **264,** 4318–4321
16. Dominici, P., Scholz, G., Kwok, F., and Churchich, J. E. (1988) *J. Biol. Chem.* **263,** 14712–14716
17. Kwok, F., and Churchich, J. E. (1991) *Eur. J. Biochem.* **199,** 157–162
18. Wolkers, W. F., Gregory, J. D., Churchich, J. E., and Serpersu, E. H. (1991) *J. Biol. Chem.* **266,** 20761–20766
19. Arnone, A., Rogers, P., Scholz, G., and Kwok, F. (1989) *J. Biol. Chem.* **264,** 4322–4323
20. Kwok, F., Scholz, G., and Churchich, J. E. (1987) *Eur. J. Biochem.* **168,** 577–583
21. Churchich, J. E., and Wu, C. (1981) *J. Biol. Chem.* **256,** 780–784
22. Sigrell, J. A., Cameron, A. D., Jones, T. A., and Mowbray, S. L. (1998) *Structure* **6,** 183–193
23. Sigrell, J. A., Cameron, A. D., and Mowbray, S. L. (1999) *J. Mol. Biol.* **290,** 1009–1018
24. Schumacher, M. A., Scott, D. M., Mathews, I. I., Ealick, S. E., Roos, D. S., Ullman, B., and Brennan, R. G. (2000) *J. Mol. Biol.* **298,** 875–893
25. Cheng, G., Bennett, E. M., Begley, T. P., and Ealick, S. E. (2002) *Structure* **10,** 225–235
26. Li, M. H., Kwok, F., An, X. M., Chang, W. R., Lau, C. K., Zhang, J. P., Liu, S. Q., Leung, Y. C., Jiang, T., and Liang, D. C. (2002) *Acta Crystallogr. Sect. D Biol. Crystallogr.* **58,** 1479–1481
27. Otwinowski, Z. (1993) in *Proceedings of the CCP4 Study Weekend* (Issacs, N., Bailey, S., and Sawyer, L., eds) pp. 56–62, Daresbury Laboratories, Warrington, UK
28. Otwinowski, Z. (1991) *Isomorphous Replacement and Anomalous Scattering* (Wolf, W., Evans, P. R., and Leslie, A. G. W., eds) pp. 80–86, SERC Daresbury Laboratory, Warrington, UK
29. Lu, G. (1999) *J. Appl. Crystallogr.* **32,** 365–368
30. Cowtan, K., and Main, P. (1998) *Acta Crystallogr. Sect. D Biol. Crystallogr.* **54,** 487–493
31. Jones, T. A., Zuo, J. Y., Cowan, S. W., and Kjeldgaard, M. (1991) *Acta Crystallogr. Sect. A* **47,** 110–119
32. Brunger, A. T., Adams, P. D., Clore, G. M., DeLano, W. L., Gros, P., Grosse-Kunstleve, R. W., Jiang, J. S., Kuszewski, J., Nilges, M., Pannu, N. S., Read, R. J., Rice, L. M., Simonson, T., and Warren, G. L. (1998) *Acta Crystallogr. Sect. D Biol. Crystallogr.* **54,** 905–921
33. Laskowski, R. A., MacArthur, M. W., Moss, D. S., and Thornton, J. M. (1993) *J. Appl. Crystallogr.* **26,** 283–291
34. Mathews, I. I., Erion, M. D., and Ealick, S. E. (1998) *Biochemistry* **37,** 15607–15620
35. Campobasso, N., Mathews, I. I., Begley, T. P., and Ealick, S. E. (2000) *Biochemistry* **39,** 7868–7877
36. Ito, S., Fushinobu, S., Yoshioka, I., Koga, S., Matsuzawa, H., and Wakagi, T. (2001) *Structure* **9,** 205–214
37. Laine-Cessac, P., and Allain, P. (1996) *Enzyme Protein* **49,** 291–304
38. Kraulis, P. J. (1991) *J. Appl. Crystallogr.* **24,** 946–950
39. Merrit, E. A., and Murphy, M. E. P. (1994) *Acta Crystallogr. D* **50,** 869–873
40. Nicholl, A., Sharp, K., and Honig, B. H. (1991) *Proteins* **11,** 281–296
41. Jones, T. A. (1978) *J. Appl. Crystallogr.* **11,** 268–272